Sharp hemisphere boundaries in a translating inner core

Z. M Geballe, M. Lasbleis, V. F Cormier, E. A Day

HAL Id: hal-02308892
https://hal.science/hal-02308892

Submitted on 8 Oct 2019

Sharp hemisphere boundaries in a translating inner core

Z. M. Geballe,[1] M. Lasbleis,[2] V. F. Cormier,[3] and E. A. Day[4]

[1]   Geodynamic models of a convectively translating inner core have recently been proposed that would account for the seismically observed differences in isotropic velocity between the eastern and western hemispheres of the inner core. These models, however, have previously been thought to be incompatible with seismic observations of a 1.5% P wave velocity change occurring over an 800 km wide region at the boundary between hemispheres of the inner core. Here we show that if rigid translation occurs, the age of material in the 100 km below the inner core boundary changes quickly as it crosses the boundary between the western and eastern hemispheres. We then forward model seismic traveltimes to show that the sharp transition in V_P between hemispheres may be explained by a random distribution of highly oriented crystalline domains that grow during translation and are composed of material with relatively high elastic anisotropy (up to 12%). **Citation:** Geballe, Z. M., M. Lasbleis, V. F. Cormier, and E. A. Day (2013), Sharp hemisphere boundaries in a translating inner core, *Geophys. Res. Lett.*, *40*, doi:10.1002/grl.50372.

1.   Introduction

[2]   Study of the Earth's inner core provides unique insights into the evolution of our planet, as well as the processes that are occurring deep within the Earth today. The inner core is likely to play a crucial role in generating the modern day geodynamo by releasing light elements [*Lister and Buffett*, 1995], and it may stabilize the polarity of the Earth's magnetic field [*Glatzmaier and Roberts*, 1995]. Yet basic properties remain poorly constrained, including the age, composition, viscosity, and temperature of the inner core [*Sumita and Bergman*, 2007].

[3]   Seismology provides crucial constraints on the evolution of the inner core, despite only providing a snapshot of the inner core as it is today. Early seismic body wave [*Morelli et al.*, 1986] and normal mode [*Woodhouse et al.*, 1986] studies revealed elastic anisotropy, which motivated models of lattice preferred orientation due to convection

[*Jeanloz and Wenk*, 1988; *Weber and Machetel*, 1992], or due to Maxwell stresses [*Karato*, 1999]. More refined studies of inner core P waves revealed a degree one structure, with the western hemisphere being substantially more anisotropic than the east [*Tanaka and Hamaguchi*, 1997; *Irving and Deuss*, 2011]. The uppermost ∼100 km of both hemispheres were seen to be isotropic, but not the same: the P wave velocity in the western hemisphere is ∼1% slower [*Niu and Wen*, 2001; *Waszek and Deuss*, 2011], but attenuation is smaller than in the east [*Niu and Wen*, 2001; *Cao and Romanowicz*, 2004]. This implies a negative correlation between V_P and Q, whereas the Earth's mantle has a positive correlation [*Roth et al.*, 2000].

[4]   Some recent geodynamical models explain the seismically observed hemispherical dichotomy by the convective translation of the inner core, together with a grain growth model and a scattering model of seismic wave propagation [*Monnereau et al.*, 2010; *Alboussière et al.*, 2010]. Dynamically, they propose that solid material is convected through the inner core from the western to the eastern side of the inner core boundary, where it melts and is entrained into the outer core. The melt may stagnate near the inner core boundary, providing iron-rich material that could explain the seismological F layer [*Alboussière et al.*, 2010]. Within the inner core, material on the western side is younger, suggesting smaller domains of preferentially oriented crystals. The smaller domains may explain observations of reduced velocities and lower attenuations in the isotropic upper region of the west, according to certain models of seismic wave propagation in polycrystalline material [*Monnereau et al.*, 2010].

[5]   A simple translating model of the inner core, however, does not seem to explain all of the seismically observed features, including the innermost inner core [*Cormier and Li*, 2002; *Ishii and Dziewoński*, 2002] and the complex hemispherical and radial dependence of anisotropy, attenuation, and scattering in the uppermost inner core [*Cormier*, 2007; *Waszek et al.*, 2011]. Most recently, the translation model has been criticized for failing to explain the sharpness of the boundary between the two hemispheres inferred from P wave traveltime variations in the uppermost inner core [*Waszek and Deuss*, 2011].

[6]   Here we test the compatibility of simple models of a convectively translating inner core with published seismic data of the upper ∼100 km of the inner core. First, we calculate the age of material in different regions sampled by PKiKP-PKIKP seismic data, focusing on the boundary between the two hemispheres. We then compare our predicted traveltime residuals to the binned traveltime residuals of *Waszek and Deuss* [2011], which showed an abrupt change in seismic properties at the boundary between the two hemispheres. By considering many sets of elastic constants, we are able to find one model of iron that reproduces the abrupt change in isotropic velocity, while five do not.

[1]Department of Earth and Planetary Science, University of California Berkeley, Berkeley, California, USA.

[2]Laboratoire de Géologie de Lyon, École Normale Supérieure de Lyon, Université de Lyon, CNRS, Lyon, France.

[3]Department of Physics, University of Connecticut, Storrs, Connecticut, USA.

[4]Department of Earth, Atmospheric and Planetary Sciences, Massachusetts Institute of Technology, Cambridge, Massachusetts, USA.

Corresponding author: Z. M. Geballe, Department of Earth and Planetary Science, University of California Berkeley, Berkeley, CA 94720, USA. (zgeballe@berkeley.edu)
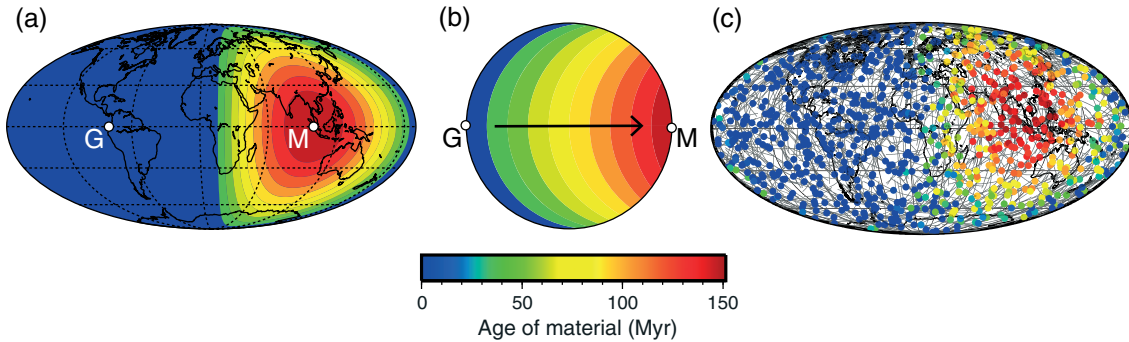
Figure 1. Age contours on the (a) surface and on a (b) vertical cross section of the inner core, assuming a rigid translation at 16 km/Myr along the vector connecting the center of the western hemisphere (−80°, 0°) to center of the eastern hemisphere (100°, 0°). (c) Forward models of 1000 random raypaths of PKIKP waves bottoming at a uniform distribution of depths between 15 and 106 km below the inner core boundary, the depth range sampled by the data set of *Waszek and Deuss* [2011]. The raypaths in the inner core are shown by gray lines, and the continents are projected onto the inner core surface in both Figures 1a and 1c. The turning points of the rays in the inner core are denoted by circles; the colors indicate the ages of the material sampled by the ray at its bottoming depth and show a hemispherical dichotomy.

2. Age of Material in a Translating Inner Core

[7] If the inner core is convectively translating, then the age of material since its time of crystallization varies as a function of distance from the crystallizing hemisphere. Following the proposal of *Monnereau et al.* [2010], we assume the inner core translates from west to east, where west is defined as the hemisphere centered at 0° latitude, −80° longitude (marked by G on Figure 1a). We consider a translation rate of 16 km/Myr; consequently, the inner core renews itself every 150 Myr, as has been suggested in *Alboussière et al.* [2010]. Since the timescale of inner core growth is likely an order of magnitude longer, we make the simplifying assumption that the net growth rate is zero.

[8] The age of any point in the inner core is its distance from the crystallizing western hemisphere of the inner core boundary (ICB) divided by the translation velocity:

$$\text{Age} = D/v_{\text{trans}}, \tag{1}$$

where the distance, D, is given by

$$D = \sqrt{r'^2_{\text{ICB}} - r'^2 \sin^2(\phi + 80°)} - r' \cos(\phi + 80°), \tag{2}$$

[9] where $r'_{\text{ICB}} = \sqrt{r^2_{\text{ICB}} - r^2 \sin^2 \theta}$ is the radius of a horizontal slice of the inner core at (r, θ, ϕ), and $r' = r \cdot \cos \theta$ is the radius to a point (r, θ, ϕ) projected onto the same slice. Age varies gradually from west to east in a cross section of the inner core (Figure 1a), but it varies sharply along the surface of the inner core (Figure 1b).

[10] In order to compare to seismic data, we calculate the age of material sampled in a translating inner core by a random set of 1000 paths through the inner core, which turn at between 15 and 106 km depth below the ICB (mimicking the path of PKIKP through the inner core). The calculated ages of the 1000 random turning points are shown in Figure 1c. In Figure 2, the same ages are plotted as a function of angular distance (i.e., great circle length) from the turning point to a point on the inner core's equator at −80° longitude. The age is roughly constant in the west and increases rapidly near the boundary between hemispheres, which suggests that the change in V_p from west to east may match the abruptness

of the change seen in the seismic data in *Waszek and Deuss* [2011].

[11] We note that at greater depths inside the inner core, the hemispherical dichotomy in age persists but is less dramatic. For example, at 700 km depth below the ICB, the age of material along the equator increases with longitude from 40 Myr at (−80°, 0°), to 50 Myr at (−20°, 0°), to 90 Myr at (40°, 0°), and finally to 110 Myr at (100°, 0°). For comparison, the ages along the equator of the inner core boundary are 0 Myr, 0 Myr, 80 Myr, and 150 Myr at the same longitudes. Further work is needed to determine whether the persistence of hemispherical differences is incompatible with seismic observations of the innermost inner core.

3. Evolution of Seismic Properties with Age

[12] To calculate seismic properties as a function of age of material in the inner core, we first assume a model for the growth of highly oriented crystalline domains (referred to as "patches" in *Calvet and Margerin* [2008]). They can be made of many single crystals, as long as crystallographic axes are preferentially aligned with one another. In the absence of shear forces that break and rotate crystals significantly (e.g., during a purely rigid translation of the inner core), the growth of domains should follow a crystal growth scaling relationship. Following *Bergman et al.* [2010], we assume that domain size, a, is a function of grain boundary mobility, M, surface energy, γ, and age, t: $a = (M\gamma t)^{1/2}$. For the remainder of the paper, we assume $M \cdot \gamma = 8 \cdot 10^{10}$ m²/s. Figure 2b shows the resulting distribution of domain sizes for the same set of points between 15 and 106 km depth below the ICB used to generate Figure 1.

[13] The value of $M \cdot \gamma$ is poorly constrained by laboratory data: it can range over 8 orders of magnitude [*Bergman et al.*, 2010]. The value chosen here is therefore feasible but not independently constrained. Our choice is dictated by the goal of matching the large spatial variation in V_P that is seismically observed.

[14] Finally, we must choose an elastic wave propagation model for 1 Hz seismic waves traveling through inner core material of varying domain sizes. As in *Monnereau et al.* [2010], we assume the multiple scattering theory of
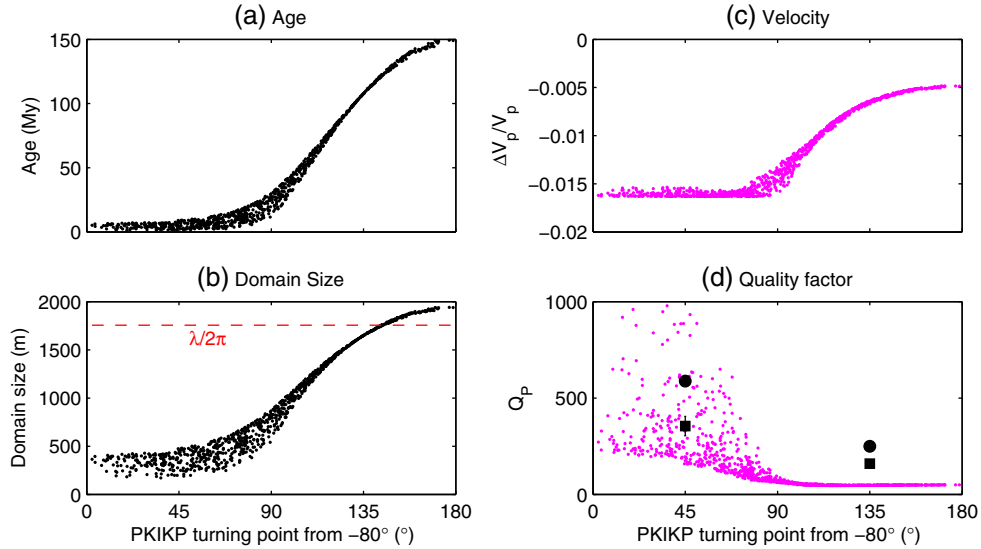
Figure 2. Modeled values of (a) age since crystallization, (b) domain size, (c) average velocity anomaly, and (d) quality factor as a function of distance from the point (−80°, 0°). In Figure 2d, Q_P values inferred for the east and west from seismological studies of *Cao and Romanowicz* [2004] and of *Wen and Niu* [2002] are indicated by black squares and circles, respectively. Age is calculated by equations (1) and (2). Then domain size is calculated by the chosen grain growth model. Finally, velocity and attenuation are calculated by the multiple scattering model described in section 3.

Calvet and Margerin [2008], which models velocity dispersion and attenuation in a polycrystalline aggregate of randomly oriented anisotropic crystals of a single phase. The single-crystal-like domains are assumed to vary in size according to the correlation function $e^{-\Delta r/a}$, where Δr is the distance between any two points.

[15] Assuming one particular model of iron's elasticity, *P* wave velocity and attenuation are shown in Figures 2c and 2d. We compute seismic properties as a function of position by multiplying the domain size, *a* (Figure 2b), by the wave number of a 1 Hz seismic wave, $k = 2\pi/11$ km^{-1}, and reading the value of velocity and attenuation from Figures 3 and 4 of *Calvet and Margerin* [2008]. Next, the average velocity and attenuation along each seismic raypath are calculated by averaging slowness (V_P^{-1}) and attenuations (Q_P^{-1}), respectively.

[16] Figure 2d shows that the trend in seismically derived values of Q_P for the upper 100 to 200 km of the eastern and western hemispheres (black symbols) is consistent with the model proposed here (pink dots), but that our values of Q_P in the east are smaller than the seismically derived values by a factor of ∼3 to 5 [*Cao and Romanowicz*, 2004; *Wen and Niu*, 2002]. The calculated attenuation only accounts for scattering, not viscoelastic attenuation. Therefore, the true values of Q_P are less than or equal to the values plotted in Figure 2d, enhancing the disagreement between model and observation.

[17] The traveltime residuals from this elasticity and translation model match the PKiKP-PKIKP traveltime residuals from *Waszek and Deuss* [2011] to within the standard deviation of their data (Figure 3), showing that sharp hemisphere boundary in isotropic velocity can be compatible with translation. Model traveltimes are calculated as the path length divided by $(\Delta Vp/Vp) \cdot Vp_{\mathrm{IC}}$ for the velocity at the top of the inner core, $Vp_{\mathrm{IC}} = 11$ km/s. The scatter in modeled traveltimes is large compared to the narrow range of seismic

velocities presented in Figure 2c, a result of multiplying by path length, which varies from 380 km to 1000 km for rays bottoming at 15 km to 106 km depth.

[18] Figure 4 shows that the model of *Belonoshko et al.* [2007] is the only one of the six elasticity models of iron presented in *Calvet and Margerin* [2008] that matches the magnitude of variation in observed traveltime residuals from west to east. The elastic anisotropy of the other models is too weak to cause large impedance mismatches across grain boundaries, reducing the probability of a wave scattering, and resulting in limited variation in velocity as a function of *ka* (by less than 0.6% in Figure 3 of *Calvet and Margerin* [2008]).
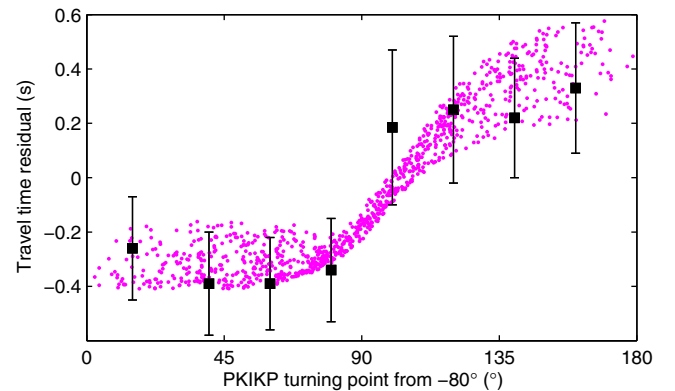
Figure 3. Observed traveltime residuals of *Waszek and Deuss* [2011] (black squares) are similar to the calculated residuals for the model proposed in this study (pink dots). Black squares and their error bars indicate the averages and standard deviations of binned traveltime residuals observed in *Waszek and Deuss* [2011].

3
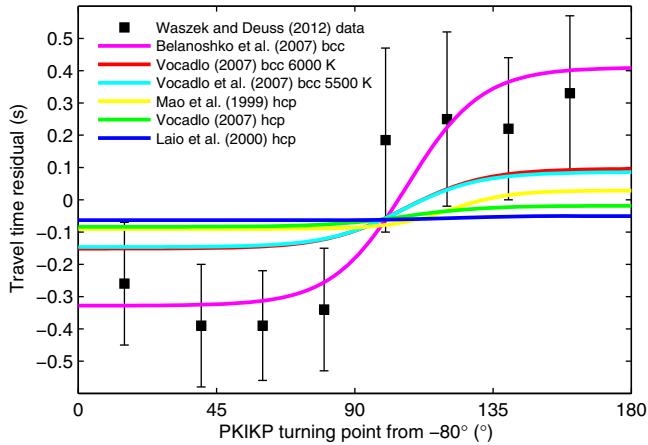
Figure 4. Predicted *P* wave traveltime residuals for a range of elastic models of iron are compared to the real seismic measurements of *Waszek and Deuss* [2011]. The six colored curves are sigmoidal fits to forward modeled seismic traveltime residuals assuming the distribution of domain sizes described in the text, and modeling *P* wave velocity anomalies by assuming the six different models of iron's elasticity used in *Calvet and Margerin* [2008]. The sigmoid used here is $c + A \cdot \tanh((d - d0)/\sigma)$, where *d* is the distance of the PKIKP turning point from $-80°$ and $d0$, σ, *A*, and *c* are fitting parameters. The only model to match the ~ 0.7 s step in traveltime residual from western to eastern hemispheres assumes the highly anisotropic elasticity of bcc iron from *Belonoshko et al.* [2007].

[19] To maximize the variation in velocity from west to east, we tuned our choice of crystal growth rate so that domains grow to roughly $\lambda/2\pi$ for the seismic wavelength $\lambda = 11$ km at 1 Hz, causing the nondimensional frequency, *ka*, to increase from below 1 to above 1. Our search for an elasticity model is more limited. The velocity anisotropy of single crystals of both hcp and bcc iron is still in dispute at core conditions [*Deguen*, 2012], and the effect of light elements is unknown. So, it is feasible that either crystal structure could have large enough anisotropy to create the large dispersion in isotropic velocity as a function of *ka* that is required to fit traveltime residual data.

[20] With a slightly different set of assumptions, *Monnereau et al.* [2010] carried out a search of elastic constants for hcp iron and found that the hemispherical variations in both V_p and *Q* can be fitted using the multiple scattering model of *Calvet and Margerin* [2008]. The seismic constraints they fit are a V_P difference between $(-80°, 0°)$ and $(100°, 0°)$ of $1.5 \pm 0.5\%$, $Q_P = 423 \pm 114$ in the west, and $Q_P = 168 \pm 45$ in the east.

4. Discussion

[21] We predict that the age of material sampled by PKIKP will change abruptly as its turning point varies across the boundary between the two hemispheres of a translating inner core (Figure 2a). Assuming that the age of material acts as a proxy for seismic properties (as it does in our modeling), this will also correspond to a sharp hemisphere boundary, as observed in *Waszek et al.* [2011] and *Waszek and Deuss* [2011]. Such an abrupt change was previously interpreted as evidence against translation [*Waszek and Deuss*, 2011], but

we have found the opposite: a sharp boundary is consistent with a translating inner core.

[22] We have also matched the trend, basic shape, and magnitude of the previously observed isotropic velocity variation between hemispheres [*Waszek and Deuss*, 2011] by applying the grain growth model of *Bergman et al.* [2010] and the wave propagation model of *Calvet and Margerin* [2008]. Since the source of V_P variation is dispersion of velocity (i.e., V_P is a function of *ka*), an eastward translation of the inner core is required here, as younger material has a smaller domain size, *a*, and is therefore seismically slower than the older material.

[23] Nonetheless, we note that an abrupt change in the average age of material sampled would occur independent of the direction of translation. A westward translation of the inner core, as proposed by *Aubert* [2013], would still result in an abrupt change in age between the hemispheres; the trend in Figure 2a would simply appear reflected about a vertical line at 90°. Should the translation direction have changed in the geologically recent past, this may have affected outer core convection, but not yet affected the observable seismic properties of the inner core [*Olson and Deguen*, 2012; *Aubert*, 2013].

[24] Despite our success at recreating the sharp hemisphere boundary observed in isotropic velocity by *Waszek and Deuss* [2011], a number of additional features of the inner core are not well explained by this simple translation model. For example, in a steadily translating inner core scenario, hemispherical variations in age persist (though with reduced magnitude) to the inner 500 km of the core. Furthermore, the anisotropy observed in some regions may not be compatible with the grain growth model applied here: extensive grain growth requires low shear forces, whereas anisotropy is commonly explained by texturing caused by shear forces. Nevertheless, it may be possible to reconcile the innermost inner core with a modified translation model in which a period of convection within the inner core is followed by a period of translation.

[25] Motivated by the modest success of the translation model in this study, we suggest two further tests for the future. Following the success of velocity dispersion in explaining hemispherical variations in V_P, we propose a search for frequency dependence of V_P within each hemisphere. Given the usefulness of multiple scattering theory in explaining heterogeneity in both V_P and Q_P, we propose a modeling effort to describe the scattering of seismic waves through a textured mixture of anisotropic crystals. This would allow inner core anisotropy and heterogeneity to be forward modeled simultaneously.

[26] While convective translation of the inner core remains an uncertain hypothesis, we have seen that it is consistent with seismic data that have previously been interpreted as evidence against translation, motivating us to propose further tests of the hypothesis.

5. Conclusions

[27] A hemispherical boundary that appears sharp, with a very abrupt change in isotropic velocity from the western to the eastern hemisphere of the uppermost inner core, is compatible with models of a translating inner core. The source of the abrupt change modeled here is that the age of material in the uppermost 110 km of the inner core increases

dramatically across the hemisphere boundary. To quantitatively match the *P* wave traveltimes from *Waszek and Deuss* [2011], oriented crystalline domains must grow to several kilometers in size and a relatively anisotropic single crystal elasticity model must be employed. One of the six proposed models of iron's elasticity tested here predicts the sign and magnitude of the observed variation in isotropic *P* wave velocity, as well as the sign of the change in attenuation between hemispheres.

References

Alboussière, T., R. Deguen, and M. Melzani (2010), Melting-induced stratification above the Earth's inner core due to convective translation., *Nature*, *466*, 744–747, doi:10.1038/nature09257.

Aubert, J. (2013), Flow throughout the earth's core inverted from geomagnetic observations and numerical dynamo models, *Geophys. Journ. Int.*, *192*, 537–556, doi:10.1093/gji/ggs051.

Belonoshko, A. B., N. V. Skorodumova, S. Davis, A. N. Osiptsov, A. Rosengren, B. Johansson (2007), Origin of the low rigidity of the Earth's inner core, *Science*, *316*, 1603–1605, doi:10.1126/science.1141374.

Bergman, M. I., D. J. Lewis, I. H. Myint, L. Slivka, S.-I. Karato, and A. Abreu (2010), Grain growth and loss of texture during annealing of alloys, and the translation of Earth's inner core, *Geophys. Res. Lett.*, *37*, L22,313, doi:10.1029/2010GL045103.

Calvet, M., and L. Margerin (2008), Constraints on grain size and stable iron phases in the uppermost inner core from multiple scattering modeling of seismic velocity and attenuation, *Earth Planet. Sci. Lett.*, *267*, 200–212, doi:10.1016/j.epsl.2007.11.048.

Cao, A., and B. Romanowicz (2004), Hemispherical transition of seismic attenuation at the top of the Earth's inner core, *Earth Planet. Sci. Lett.*, *228*, 243–253, doi:10.1016/j.epsl.2004.09.032.

Cormier, V. F. (2007), Texture of the uppermost inner core from forward- and back-scattered seismic waves, *Earth Planet. Sci. Lett.*, *258*, 442–453, doi:10.1016/j.epsl.2007.04.003.

Cormier, V. F., and X. Li (2002), Frequency-dependent seismic attenuation in the inner core 2. A scattering and fabric interpretation, *J. Geophys. Res.*, *107*(B12), ESE 14-1 - ESE 14-15, doi:10.1029/2002JB001796.

Deguen, R. (2012), Structure and dynamics of Earth's inner core, *Earth Planet. Sci. Lett.*, *333-334*, 211–225, doi:10.1016/j.epsl.2012.04.038.

Glatzmaier, G. A., and P. H. Roberts (1995), A three-dimensional convective dynamo solution with rotating and finitely conducting inner core and mantle, *Phys. Earth Planet. Inter.*, *91*, 63–75.

Irving, J. C. E., and A. Deuss (2011), Hemispherical structure in inner core velocity anisotropy, *J. Geophys. Res.*, *116*, B04,307, doi:10.1029/2010JB007942.

Ishii, M., and A. M. Dziewoński (2002), The innermost inner core of the earth: Evidence for a change in anisotropic behavior at the radius of about 300 km, *Proc. Natl. Acad. USA*, *99*, 14,026–14,030, doi:10.1073/pnas.172508499.

Jeanloz, R., and H.-R. Wenk (1988), Convection and anisotropy of the inner core, *Geophys. Res. Lett.*, *15*, 72–75.

Karato, S.-I. (1999), Seismic anisotropy of the Earth's inner core resulting from flow induced by Maxwell stresses, *Nature*, *402*, 871–873.

Lister, J. R., and B. A. Buffett (1995), The strength and efficiency of thermal and compositional convection in the geodynamo, *Phys. Earth Planet. Inter.*, *9201*(95), 17–30.

Monnereau, M., M. Calvet, L. Margerin, and A. Souriau (2010), Lopsided growth of Earth's inner core, *Science*, *328*(5981), 1014–1017, doi:10.1126/science.1186212.

Morelli, A., A. M. Dziewoński, and J. H. Woodhouse (1986), Anisotropy of the inner core inferred from PKIKP travel times, *Geophys. Res. Lett.*, *13*, 1545–1548.

Niu, F., and L. Wen (2001), Hemispherical variations in seismic velocity at the top of the Earth's inner core, *Nature*, *410*, 1081–1084, doi:10.1038/35074073.

Olson, P., and R. Deguen (2012), Eccentricity of the geomagnetic dipole caused by lopsided inner core growth, *Nature Geosci.*, *5*, 565–569, doi:10.1038/NGEO1506.

Roth, E. G., D. A. Wiens, and D. Zhao (2000), An empirical relationship between seismic attenuation and velocity anomalies in the upper mantle, *Geophys. Res. Lett.*, *27*, 601–604.

Sumita, I., and M. I. Bergman (2007), Inner-core dynamics, in *Treatise on Geophysics*, vol. 8, edited by G. Schubert, pp. 299–318, Elsevier.

Tanaka, S., and H. Hamaguchi (1997), Degree one heterogeneity and hemispherical variation of anisotropy in the inner core from PKP(BC)-PKP(DF times, *J. Geophys. Res.*, *102*(B2), 2925–2938.

Waszek, L., and A. Deuss (2011), Distinct layering in the hemispherical seismic velocity structure of Earth's upper inner core, *J. Geophys. Res.*, *116*, B12,313, doi:10.1029/2011JB008650.

Waszek, L., J. Irving, and A. Deuss (2011), Reconciling the hemispherical structure of Earth's inner core with its super-rotation, *Nature Geosci.*, *4*, 264–267, doi:10.1038/ngeo1083.

Weber, P., and P. Machetel (1992), Convection within the inner-core and thermal implications, *Geophys. Res. Lett.*, *19*(21), 2107–2110.

Wen, L., and F. Niu (2002), Seismic velocity and attenuation structures in the top of the Earth's inner core, *J. Geophys. Res.*, *107*(B11), ESE 2-1 - ESE 2-13, doi:10.1029/2001JB000170.

Woodhouse, J. H., D. Giardini, and X.-D. Li (1986), Evidence for inner core anisotropy from free oscillations, *Geophys. Res. Lett.*, *13*, 1549–1552.